



Human Dermcidin Protects Mice Against Hepatic Ischemia-Reperfusion-Induced Local and Remote Inflammatory Injury

Xiaoling Qiang^{1,2}, Jianhua Li¹, Shu Zhu^{1,2}, Mingzhu He¹, Weiqiang Chen^{1,2}, Yousef Al-Abed^{1,2}, Max Brenner^{1,2,3}, Kevin J. Tracey^{1,2}, Ping Wang^{1,2,3†} and Haichao Wang^{1,2*†}

OPEN ACCESS

Edited by:

Pietro Ghezzi,
Brighton and Sussex Medical School,
United Kingdom

Reviewed by:

Christoph Thiemermann,
Queen Mary University of London,
United Kingdom
Charles Dinarello,
University of Colorado Denver,
United States

*Correspondence:

Ping Wang
pwang@northwell.edu
Haichao Wang
hwang@northwell.edu

†These authors have contributed
equally to this work and share
senior authorship

Specialty section:

This article was submitted to
Inflammation,
a section of the journal
Frontiers in Immunology

Received: 23 November 2021

Accepted: 24 December 2021

Published: 14 January 2022

Citation:

Qiang X, Li J, Zhu S, He M,
Chen W, Al-Abed Y, Brenner M,
Tracey KJ, Wang P and Wang H
(2022) Human Dermcidin Protects
Mice Against Hepatic Ischemia-
Reperfusion-Induced Local and
Remote Inflammatory Injury.
Front. Immunol. 12:821154.
doi: 10.3389/fimmu.2021.821154

¹ The Feinstein Institutes for Medical Research, Northwell Health, Manhasset, NY, United States, ² Donald and Barbara Zucker School of Medicine at Hofstra/Northwell, Hempstead, NY, United States, ³ TheraSource LLC, Manhasset, NY, United States

Background: Hepatic ischemia and reperfusion (I/R) injury is commonly associated with surgical liver resection or transplantation, and represents a major cause of liver damage and graft failure. Currently, there are no effective therapies to prevent hepatic I/R injury other than ischemic preconditioning and some preventative strategies. Previously, we have revealed the anti-inflammatory activity of a sweat gland-derived peptide, dermcidin (DCD), in macrophage/monocyte cultures. Here, we sought to explore its therapeutic potential and protective mechanisms in a murine model of hepatic I/R.

Methods: Male C57BL/6 mice were subjected to hepatic ischemia by clamping the hepatic artery and portal vein for 60 min, which was then removed to initiate reperfusion. At the beginning of reperfusion, 0.2 ml saline control or solution of DCD (0.5 mg/kg BW) or DCD-C34S analog (0.25 or 0.5 mg/kg BW) containing a Cys (C)→Ser (S) substitution at residue 34 was injected *via* the internal jugular vein. For survival experiments, mice were subjected to additional resection to remove non-ischemic liver lobes, and animal survival was monitored for 10 days. For mechanistic studies, blood and tissue samples were collected at 24 h after the onset of reperfusion, and subjected to measurements of various markers of inflammation and tissue injury by real-time RT-PCR, immunoassays, and histological analysis.

Results: Recombinant DCD or DCD-C34S analog conferred a significant protection against lethal hepatic I/R when given intravenously at the beginning of reperfusion. This protection was associated with a significant reduction in hepatic injury, neutrophilic CXC chemokine (Mip-2) expression, neutrophil infiltration, and associated inflammation. Furthermore, the administration of DCD also resulted in a significant attenuation of remote lung inflammatory injury. Mechanistically, DCD interacted with epidermal growth factor receptor (EGFR), a key regulator of liver inflammation, and significantly inhibited hepatic I/R-induced phosphorylation of EGFR as well as a downstream signaling molecule, protein kinase B (AKT). The suppression of EGFR expression by transducing

Egfr-specific shRNA plasmid into macrophages abrogated the DCD-mediated inhibition of nitric oxide (NO) production induced by a damage-associated molecular pattern (DAMP), cold-inducible RNA-binding protein, CIRP.

Conclusions: The present study suggests that human DCD and its analog may be developed as novel therapeutics to attenuate hepatic I/R-induced inflammatory injury possibly by impairing EGFR signaling.

Keywords: dermcidin, chemokine, neutrophil, inflammation, tissue injury, EGFR

INTRODUCTION

Hepatic ischemia and reperfusion (I/R) injury is an unavoidable consequence of circulatory shock, liver resection and transplantation, and represents a major cause of post-operative hepatic dysfunction, multiple organ failure, and even morbidity (1). It begins with an initial generation of reactive oxygen and nitrogen species (ROS and RNS) by liver macrophages (i.e., Kupffer cells) within a few hours of reperfusion. This process exerts direct but moderate hepatic injury, and facilitates the infiltration of neutrophils, which release more ROS and proteases to exacerbate a cascade of inflammatory injury (2, 3). Furthermore, the generation of ROS and RNS also leads to hepatocellular death (2, 4) and consequent release of damage-associated molecular patterns (DAMPs) such as cold-inducible RNA-binding protein (CIRP) (5) and high mobility group box 1 (HMGB1) (6, 7). We and others have shown that HMGB1 (8) and CIRP (9) exacerbate liver damage in animal models of hepatic I/R, as these DAMPs can amplify a cascade of oxidative and inflammatory responses during a late stage of reperfusion (1, 10). Despite on-going efforts in developing various pharmacological modalities to reduce hepatic I/R injury, there is still an unmet need for effective therapies (11). It is thus important to develop novel strategies to modulate local and remote inflammatory responses in patients who undergo liver transplantation, surgical resections or traumatic liver injury.

Human skin contains sweat glands that can secrete a wide array of antimicrobial peptides to restrain the growth of microbial pathogens. For instance, during rigorous exercise, an antimicrobial peptide, dermcidin (DCD), is secreted by the sweat glands onto the skin surface even in the absence of inflammatory stimuli (12, 13). It was believed that the salty and slightly acidic sweat facilitated the formation of DCD channels capable of perforating bacterial membranes to instill microbial killing (14–16). After its secretion, the full-length DCD precursor (residue 20–110) can be processed by unknown proteases into shorter peptides with anti-oxidant (14, 17) or antimicrobial activities (12, 18–20). In addition to sweat glands, some immune cells (e.g., monocytes) also express DCD after viral infections (21). Recently, we demonstrated that the full-length DCD precursor attenuated the production of nitric oxide (NO) and chemokines (e.g., GRO and MCP-3) induced either by pathogen-associated molecular patterns (PAMPs such as LPS) or damage-associated molecular patterns (DAMPs such as HMGB1 and CIRP) (22). It was previously unknown, however,

how DCD or analogs affects innate immune responses to sterile injury in preclinical settings. In the present study, we sought to explore the therapeutic potential and protective mechanisms of DCD and analog in a murine model of hepatic I/R injury.

MATERIALS AND METHODS

Materials

Dulbecco's Modified Eagle's Medium (DMEM, Cat. No. 11995-065), fetal bovine serum (FBS, Cat. No. 26140079) and penicillin/streptomycin (Cat. No. 15140-122) were purchased from Invitrogen (Grand Island, New York). Recombinant mouse CIRP was expressed in *E. coli*, and purified to remove contaminating endotoxins by Triton X-114 extraction as previously described (5). Recombinant human dermcidin (corresponding to residue 20–100, without the N-terminal 19-aa leader sequence) was expressed in *E. coli* BL21 (DE3) pLysS cells as previously described (22). To explore the therapeutic potential of DCD derivatives, an analog of DCD containing a Cys (C)→Ser (S) substitution at residue 34 (DCD-C34S) was also produced in *E. coli* BL21 (DE3) pLysS and purified to homogeneity using similar procedures. Recombinant DCD or DCD-C34S analog was purified by Triton X-114 extraction to remove contaminating endotoxins as previously described (22).

Adult male C57BL/6 mice (8–9 weeks old, 20–25 g body weight) were purchased from Charles River Laboratories (Wilmington, MA), and housed in a temperature-controlled room on a 12-h light-dark cycle. Mice were fed with a standard mouse chow diet, and acclimated to the environment for 5–7 days before usage. Every attempt was made to limit the number of animals used in the present study according to the ARRIVE guidelines for reducing the number of animals in scientific research developed by the British National Centre for the Replacement, Refinement and Reduction of Animals in Research (NC3Rs). Additionally, all experiments were performed in accordance with policies of the United States' National Institutes of Health and the Guide for the Care and Use of Laboratory Animals, and approved by the Institutional Animal Care and Use Committee (IACUC) of the Feinstein Institutes for Medical Research.

Animal Model of Hepatic I/R

Hepatic I/R was performed in male C57BL/6 mice (8–9 weeks old, 20–25 g) as described previously (9, 23). Animals were

anesthetized by inhalation of 2-4% isoflurane, the ventral abdomen was shaved and alternately disinfected with Betadine and 70% alcohol. The animals were placed on a heating pad connected to an indwelling rectal thermometer to maintain core body temperatures of 35°C. A 1-1.5 cm midline incision was performed to expose the liver and the ligamentous attachments connecting the liver, and the diaphragm and abdominal wall were then divided to expose hepatic artery and portal vein. A vascular micro-clip was placed across the hilum containing the left and median lobes of the liver for 60 min to produce 70% ischemia, which was confirmed by the color change. Reperfusion was initiated by the release of the clamp before closing the abdomen wound with staples (wound clips). Given the undesired effects of opioid analgesics on hosts' inflammatory responses to hepatic I/R (24–26) and other insults (27, 28), we have elected to use only a single dose of buprenorphine (0.05 mg/kg, subcutaneously) around the incision site to alleviate the immediate pain caused by surgical laparotomy. Afterwards, all animals were resuscitated by a subcutaneous injection of sterile saline solution (20 ml/kg). Blood and liver tissues were collected at 24 h after the onset of reperfusion. A portion of the left lobe of the liver was preserved in 10% formalin for histopathological analysis, and the remaining tissue was stored at -80°C for quantitative analysis.

For the survival study, the remaining 30% of non-ischemic liver was resected with electrocautery at the start of reperfusion, so the hepatic I/R could cause animal lethality in this model (9, 23). Afterwards, control vehicle (saline) or solution containing purified DCD or DCD-C34S analog were given to animals intravenously *via* internal jugular vein at the beginning of reperfusion, and animals were monitored for survival for up to 10 days.

Measurement of Organ Injury Markers

Blood samples were harvested at 24 h post the onset of reperfusion, and centrifuged at 3000 x g for 10 min to collect serum. Serum levels of liver injury markers such as alanine aminotransferase (ALT, Cat. No. 7526), aspartate aminotransferase (AST, Cat. No. 7561) and lactate dehydrogenase (LDH, Cat. No. 7572) were determined using specific colorimetric enzymatic assays (Pointe Scientific, Canton, MI) as per the manufacturer's instructions.

Measurement of Cytokines

Mice were sacrificed at 24 h post the onset of reperfusion, and liver tissues were collected to measure TNF, IL-6, and IL-1 β levels using commercial enzyme-linked immunosorbent assay (ELISA) kits (BioSource International, Camarillo, CA) as per the manufacturer's instruction.

Measurement of Nitric Oxide

The levels of nitric oxide (NO) in the liver tissue lysate or culture medium were determined by measuring the NO²⁻ production based on the colorimetric Griess reaction (29, 30). The NO²⁻ concentrations were deduced with reference to standard curves of sodium nitrite generated at various dilutions.

Assessment of Hepatic Granulocyte Myeloperoxidase

Ischemic liver tissue (100 mg) was weighed and homogenized by sonication in 1 ml of potassium phosphate buffer containing 0.5% hexadecyltrimethylammonium bromide. Two freeze-thaw cycles were performed and then samples were centrifuged to collect the supernatant. Neutrophil accumulation within the liver was then estimated using the myeloperoxidase (MPO) activity assay based on the MPO-catalyzed chemical reaction that converted O-dianisidine dihydrochloride and H₂O₂ into colorimetric product detectable by light absorbance at 460 nm over a period of 5 min. The MPO levels were expressed as units per gram of tissue per minute.

Immunohistochemical Staining of Gr-1-Positive Neutrophils

Paraffin-embedded liver or lung tissue sections were dewaxed in xylene, and rehydrated in a graded series of ethanol. Briefly, the slides were heated at 95°C for 30 min in 0.92% citric acid buffer (Vector Laboratories, Burlingame, CA). After cooling, the slides were incubated with 2% H₂O₂/60% methanol, and blocked in Tris-buffered saline containing 10% rabbit serum. The anti-Gr-1 antibody (BioLegend, San Diego, CA) was applied and incubated overnight. The detection was carried out using the NovaRED substrate of an immunohistochemistry kit (Vector Laboratories). Gr-1 positive neutrophils were counted under a high-power field microscopy (HPF; \times 200) of 4 randomly selected areas. The number of neutrophils per HPF was determined by averaging the counts of 4 HPFs.

Measurement of Cytokine mRNA by Real-Time RT-PCR

Total RNA was extracted from ischemic liver tissue using TRIzol Reagent Kit as per the manufacturer's instructions (Invitrogen, Thermo Fisher Scientific Inc.), and was reverse-transcribed into the first-strand cDNA using the RevertAidTM First Strand cDNA Synthesis Kit (Applied Biosystems, Thermo Fisher Scientific Inc.). Following reverse transcription, a panel of primers for murine iNOS, Mip-2, and β -actin were used to quantify the mRNA expression levels of respective genes using an ABI 7900HT Fast Real-time PCR system (Applied Biosystems, Foster City, CA). The sequence of primers for this study is listed as follows: mouse iNOS, 5'-GGCAAACCCAAGGTCTACGTT-3' (forward) and 5'-GAGCACGCTGAGTACCTCATTG-3' (reverse); mouse Mip-2, 5'-CCCTGGTTCAGAAAATCATCCA-3' (forward) and 5'-GCTCCTCCTTTCCAGGTCACT-3' (reverse); mouse β -actin, 5'-CGTGAAAAGATGACCCAGATCA-3' (forward) and 5'-TGGTACGACCAGAGGCATACAG-3' (reverse). Amplification was performed using the RT² SYBR Green ROX qPCR Mastermix under the following conditions: 95°C 10'; followed by 40 cycles of 95°C for 15" and 60°C for 1'. The relative mRNA expression level for each gene was calculated using the following formula: $\Delta\Delta C_t$ expression = 2^{- $\Delta\Delta C_t$} , where $\Delta\Delta C_t$ = ΔC_t (treated group) - ΔC_t (control group), ΔC_t = Ct (target gene) - Ct (β -actin), and Ct = cycle at which the threshold was reached. The relative abundance of each mRNA expression in the sham control group was set as an

arbitrary unit of 1, and the gene expression in treated groups was presented as folds of change in comparison to the sham group after normalization to β -actin.

Histological Evaluation of Liver and Lung Injury

The left lobe of liver and lung samples were harvested at 24 h post reperfusion, and fixed in 10% buffered formalin before being embedded in paraffin. Paraffin-embedded tissues were cut into 5- μ m sections, stained with hematoxylin-eosin and examined under light microscopy. As previously described (23), liver parenchymal injury was assessed in a blinded fashion by the sum of three different Suzuki scores ranging from 0-4 for sinusoidal congestion, vacuolization of hepatocyte cytoplasm, and parenchymal necrosis (23). Scores for each finding ranged from 0 to 4, with a maximum possible score of 12. The percent necrotic area was estimated by randomly evaluating 4 low-power fields (x100) of each hematoxylin-eosin-stained section using software Image J. Similarly, lung tissue sections were scored in a blinded fashion using a semi-quantitative scoring system developed by the American Thoracic Society as previously described by Matute-Bello et al. (31). As previously described (32), histological lung injury was scored based on alveolar septal thickening, as well as the presence of infiltrated inflammatory cells in the alveolar and interstitial spaces, and the presence of hyaline membranes and proteinaceous debris within airspaces according to the following definition: 0, no injury; 1, moderate injury; 2, severe injury. Using a weighted equation with a maximum score of 100 per field, the parameter scores were calculated and averaged as the final lung injury score in each experimental group.

Western Blot Analysis

Liver tissue samples were homogenized in lysis buffer (10 mM Tris-HCl pH 7.5 with 1% Triton X-100, 1 mM EDTA/EGTA, 2 mM Na₃VO₄, 0.2 mM PMSF) containing a protease inhibitor cocktail (Roche, Indianapolis, Indian). Protein concentrations were determined using DC protein assay (Bio-Rad, Hercules, CA). Equal amount of tissue homogenates or macrophage cell lysates were fractionated on SDS-PAGE and transferred to nitrocellulose membrane. The membrane was incubated with antibodies to phosphor-EGFR/EGFR or phosphor-AKT/AKT (Cell Signaling, Danvers, MA), followed by secondary antibody-horseradish peroxidase conjugate (LI-COR Biosciences). Visualization and quantification was carried out with the LI-COR Odyssey[®] scanner and software (LI-COR Biosciences).

Surface Plasmon Resonance Analysis of DCD-EGFR Interaction

We used both the newly developed Nicoya Lifesciences Open Surface Plasmon Resonance (OpenSPR) and the traditional Biacore SPR techniques to evaluate the possible DCD/EGFR interaction as previously described (32–34). In contrast to the traditional Biacore SPR that uses a continuous film of gold to detect the angle change of re-emitted light when the surface

plasmon wave interacts with a local particle, the Open SPR uses gold nanoparticles to detect small changes in the wavelength of conjugated adsorbing molecules after interacting with local ligand. For the Nicoya OpenSPR, highly purified recombinant DCD or DCD-C34S with 6 \times His Tag was immobilized on nitrilotriacetic acid (NTA) sensor chip (Cat. # SEN-Au-100-10-NTA), and recombinant EGFR corresponding to the extracellular domain (residue 25-645, Cat. No. AT#230-30016-250, RayBiotech) was applied at three different concentrations. The response signals were recorded over time, and the equilibrium dissociation constant (K_D) was estimated using the Trace Drawer Kinetic Data Analysis v.1.6.1 (Nicoya Lifesciences). For the traditional SPR, highly purified recombinant DCD was immobilized on CM5 chip (GE Healthcare), and the recombinant EGFR was applied at 5 different concentration using a Biacore T200 instrument (GE Healthcare). The K_D was determined using the Biacore evaluation software 2.0 (GE Healthcare) supposing a 1:1 binding ratio.

Knockdown of EGFR Expression in Macrophage Cultures

Murine macrophage-like RAW 264.7 cells were obtained from ATCC (ATCC, Rockville, MD), and cultured in DMEM (Invitrogen, Grand Island, New York) or RPMI 1640 (Invitrogen) supplemented with 10% heat-inactivated FBS, 1% penicillin/streptomycin and 2 mM glutamine at 37°C with 5% CO₂. To evaluate the possible role of EGFR in the regulation of DCD-mediated anti-inflammatory action, we transfected RAW 264.7 cells with lentivirus particles expressing Egfr-specific shRNAs to down-regulate EGFR expression. The use of lentivirus to express Egfr-specific shRNA in macrophages has been approved by Institutional Biosafety Committee under an IBC Registration #R-2017-007, entitled “Role of EGFR in the regulation of dermcidin-mediated anti-inflammatory action”. The lentivirus particles were produced in human kidney Lenti-X[™] 293T cells (Clontech) by co-transfer pLKO1 vector plasmid or EGFR shRNA-expression plasmid (Sigma Aldrich) together with packaging plasmids pCMV-dR8.2 dvpr and pCMV-VSV-G (Addgene) using Feugene 6 transfection agent (Promega). Lentiviral particles encoding pLKO1 vector or EGFR shRNA were harvested from medium at 48 and 72 h post-transfection, and used to transduce murine macrophage-like RAW 264.7 cells for 8 h following standard procedures. Puromycin was added to fresh culture medium every 2-3 days until resistant colonies were identified. Afterwards, adherent macrophages were gently washed with, and cultured in, DMEM before stimulation with recombinant mouse CIRP (2.0 μ g/ml) in the absence or presence of recombinant DCD for 16 h. Subsequently, the cell-conditioned culture media were analyzed for levels of nitric oxide (NO) by the Griess Reaction as previously described (35, 36).

Statistical Analysis

All experimental data were assessed for normality by using the Shapiro-Wilk test before conducting appropriate statistical tests.

For comparison among multiple groups with skewed (non-normal) distribution, the statistical differences were evaluated by using the non-parametric Kruskal-Wallis ANOVA test followed by the Dunn's *post hoc* test. For comparison among multiple groups with normal data distribution, the differences were analyzed by using the parametric one-way analyses of variance (ANOVA) followed by Fisher Least Significant Difference (LSD) *post hoc* test. For survival studies, the Kaplan-Meier method was used to compare the differences in mortality rates between groups with the nonparametric log-rank *post hoc* test. A *P* value < 0.05 was considered statistically significant.

RESULTS

Full-length DCD and DCD-C34S Analog Conferred a Significant Protection Against Lethal Hepatic I/R

As previously described (22), we generated full-length recombinant human DCD corresponding to residue 20-110 (without the signal leader peptide, residue 1-19, **Figure 1A**) in *E. coli*, and verified its purity by SDS-PAGE analysis (**Figure 1B**). Because DCD contains a Cys residue (**Figure 1A**), it could be oxidized to form an intermolecular disulfide bridge between two DCD molecules, thereby presenting DCD as a heterogeneous mixture of monomers and dimers with varying equilibrium. Consistent with previous reports (22, 37), recombinant DCD with a His-tag migrated as a 16-kDa band on SDS-PAGE gel in the presence of a reducing agent, dithiothreitol (“+DTT”) (**Figure 1B**, Left Panel), but migrated as 16-kDa and 32-kDa bands in the absence of DTT (“-DTT”), confirming that Cys (C)-containing DCD could form dimers through intermolecular disulfide cross-linking. Following extensive extraction with Triton X-114 to remove contaminating endotoxins, we tested the therapeutic efficacy of highly purified DCD in a murine model of hepatic I/R injury. Recombinant DCD conferred a significant protection against lethal hepatic I/R, increasing animal survival from 33% in the saline control to 80% in the DCD-treatment group (**Figure 1C**). Consistent with the improvement in animal survival, other pathological symptoms such as piloerection were similarly attenuated by DCD treatment (**Figure 1C**). Piloerection refers to the process of hair bristling due to involuntary contraction of piloerector muscles at the base of hair follicles, often as a reflexive response of the sympathetic nervous system to startling stimulus in an attempt to insulate hair layers to trap heat. It will thus be important to further elucidate the intricate mechanism underlying the DCD-mediated prevention of I/R-induced piloerection in future studies.

However, the development of protein therapeutics often requires the production of homogeneous peptides unable to form aggregates that could adversely trigger immunogenic responses or other side effects. Furthermore, DCD contains a single Cys residue (**Figure 1A**) that is unable to form intramolecular disulfide bridge to influence its own tertiary structure. Given the minimal structural difference between the side chains of Cys (-SH group) and Ser (-OH group, **Figure 1A**),

we generated an analog of DCD containing a Cys (C)→Ser (S) substitution at residue 34 (DCD-C34S, **Figures 1A, B**) to prevent intermolecular disulfide cross-linking. Indeed, recombinant DCD-C34S migrated as a 16-kDa monomer in SDS-PAGE gel even in the absence of a reducing agent, DTT (**Figure 1B**, Right Panel). Similarly, this DCD-C34S analog significantly increased animal survival rates when given at an identical (0.5 mg/kg BW) or a lower (0.25 mg/kg BW; **Figure 1D**) doses, confirming that DCD and DCD-C34S analog confer similar protections against lethal hepatic I/R. It also supports a therapeutic potential for the homogenous DCD-C34S analog in preclinical settings.

Intravenous DCD Administration Attenuated Hepatic I/R-Induced Liver Injury

To elucidate the mechanisms underlying DCD-mediated protection against lethal hepatic I/R, we examined the impact of DCD administration on hepatic I/R injury. At the dose that conferred protection against lethal hepatic I/R, DCD also significantly reduced hepatic I/R-induced liver injury (**Figure 2A**), as judged by the reduction in histological scores of hepatocellular necrosis, cytoplasmic vacuolization, sinusoidal congestion, and cellular infiltration at 24 h post the onset of reperfusion (**Figure 2B**). Consistently, blood levels of hepatic injury markers such as liver enzymes (AST and ALT) and LDH were also significantly reduced by DCD administration (**Figure 2C**), suggesting that DCD conferred significant protection against lethal hepatic I/R partly by attenuating I/R-induced liver injuries.

Intravenous DCD Administration Inhibited Hepatic Neutrophil Infiltration and Inflammation

To further explore the mechanisms underlying DCD-mediated protection, we further examined the effect of DCD administration on hepatic leukocyte infiltration and associated inflammation. The administration of DCD at the beginning of reperfusion resulted in a significant reduction in the expression of a neutrophilic CXC chemokine, macrophage inflammatory protein 2 (Mip-2/Cxcl2), at 24 h post reperfusion (**Figure 3A**). This suppression of Mip-2 expression was associated with a parallel reduction in the number of Gr-1-positive neutrophils infiltrated into the ischemic hepatic tissues (**Figure 3B**, Left Panel), as judged by immunohistological analysis of Gr-1-positive cells in the liver tissue (**Figure 3C**), as well as a biochemical assay of hepatic MPO enzyme activities (**Figure 3B**, Right Panel). In agreement with these findings, there was a parallel and significant reduction in the production of several proinflammatory cytokines such as TNF, IL-1 β and IL-6 in animals treated with DCD as compared with those in the saline control group (**Figure 3D**). Similarly, DCD administration also led to a significant reduction in hepatic I/R-induced production of nitric oxide (NO, **Figure 3E**, Left Panel), which was associated with a significant attenuation of the expression of inducible nitric oxide synthase (iNOS, **Figure 3E**, Right Panel). Collectively, these findings suggest that DCD promotes significant protection against

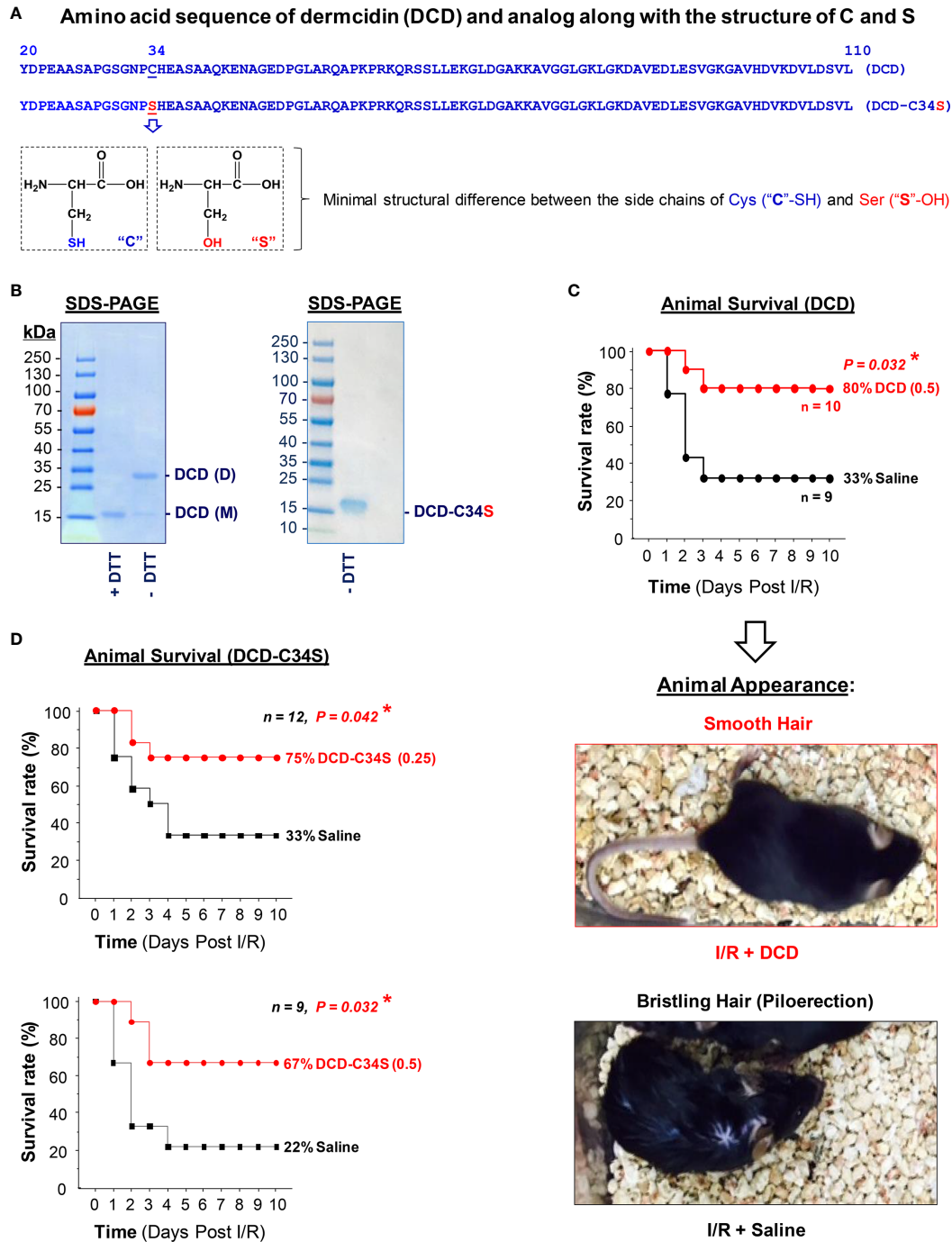


FIGURE 1 | Recombinant dermcidin (DCD) and DCD-C34S analog conferred significant protection against lethal hepatic ischemia-reperfusion injury. **(A)** Amino acid sequence of full length DCD precursor (residue 20-110) and a DCD-C34S analog containing a Cys (C)→Ser (S) substitution at residue 34. The structural difference between Cys (C) and Ser (S) was also noted. **(B)** SDS-PAGE analysis of recombinant DCD (residue 20-110) and DCD-C34S analog with an N-terminal 6×His tag. Recombinant DCD migrated as a 16-kDa monomer (M) in the presence of a reducing agent (DTT), but migrated as both a 16-kDa monomer (M) and 32-kDa dimer (D) in the absence of DTT, suggesting possible disulfide cross-linkage to form DCD dimers. In contrast, DCD-C34S analog migrated as a homogenous 16-kDa band even in the absence of DTT. **(C, D)** Highly purified DCD and DCD-C34S analog conferred significant protection against lethal hepatic ischemia-reperfusion injury. Male C57BL/6 mice were subjected to hepatic ischemia for 60 min to produce injury in 70% of the liver. At the beginning of the reperfusion, the remaining 30% of the non-ischemic liver portion was surgically resected, and 0.2 ml saline or solution containing DCD (0.5 mg/kg BW) or DCD-C34S (0.25 or 0.5 mg/kg BW) was injected via the internal jugular vein, and animals were monitored for survival for up to 10 days. The Kaplan-Meier method was used to compare the differences in mortality rates (with skewed distribution) between groups with the nonparametric log-rank *post hoc* test. **P* value < 0.05 versus "saline" control group. Representative images showed the respective absence or presence of piloerection in the DCD treatment group ("I/R + DCD") and saline control group ("I/R + Saline") at 24 h post reperfusion.

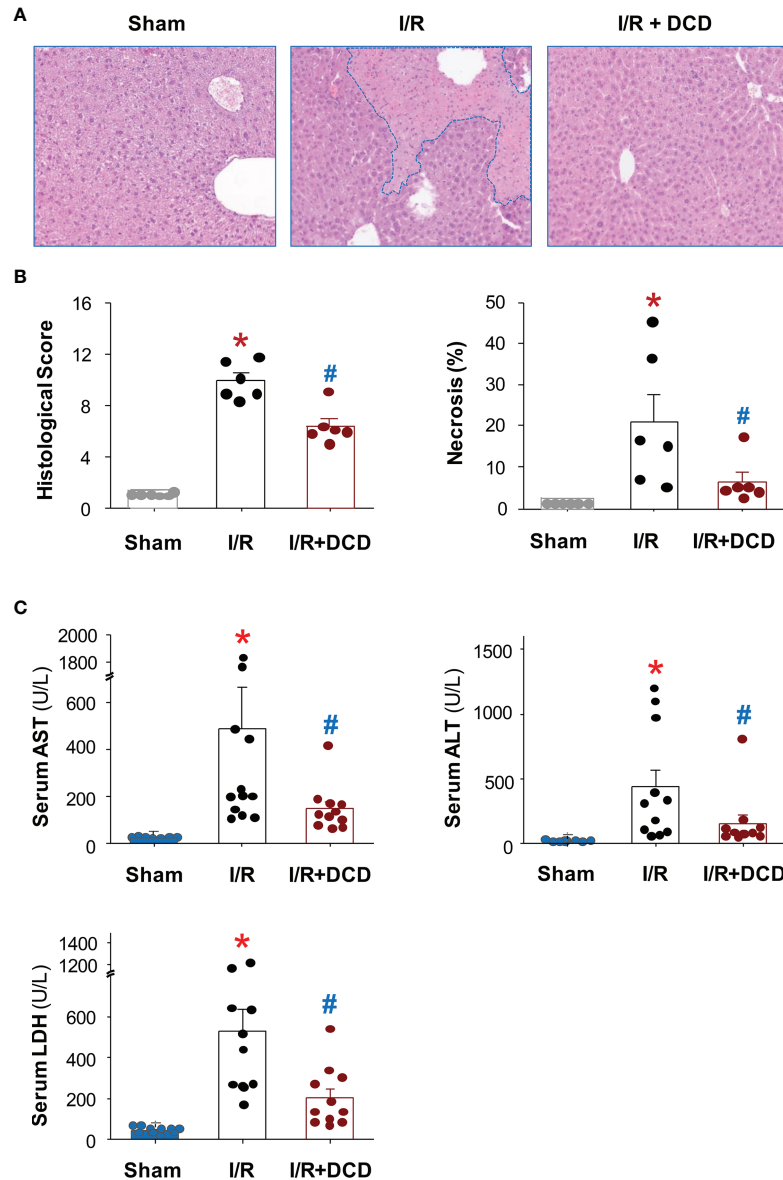


FIGURE 2 | Recombinant DCD attenuated hepatic I/R injury. Male C57BL/6 mice were subjected to hepatic ischemia for 60 min, and treated with control vehicle or DCD solution (0.5 mg/kg) at the beginning of the reperfusion. At 24 h post the onset of reperfusion, the liver tissue was subjected to histological analysis using the Suzuki liver injury scores and % of necrosis (with skewed distribution, **(A, B)**), as well as biochemical assays of liver injury markers such as alanine aminotransferase (ALT), aspartate aminotransferase (AST) and lactate dehydrogenase (LDH) using commercial kits (with skewed distribution, **(C)**). Various liver injury scores and biomarkers were expressed as means \pm SEM of 6 animals per group, and compared by Kruskal-Wallis ANOVA test followed by the Dunn's *post hoc* test. * $P < 0.05$ vs. "Sham"; # $P < 0.05$ vs. "I/R" group.

lethal hepatic I/R injury partly by attenuating I/R-induced local inflammatory responses.

Intravenous DCD Administration Led to a Significant Inhibition of Lung Neutrophil Infiltration and Injury

It is well-known that hepatic I/R injury often causes remote tissue inflammatory injury, as characterized by the induction of a

cascade of proinflammatory mediators that culminates in the recruitment of leukocytes to remote tissues (38–40). To further elucidate the mechanism underlying DCD-mediated protection, we assessed the effect of DCD administration on hepatic I/R-induced lung inflammatory injury. Consistent with previous findings (39), hepatic I/R induced marked lung inflammatory injuries as manifested by the increase in alveolar septal wall thickening, leukocyte infiltration, and alveolar congestion (**Figure 4A**). These hepatic I/R-elicited lung injuries were

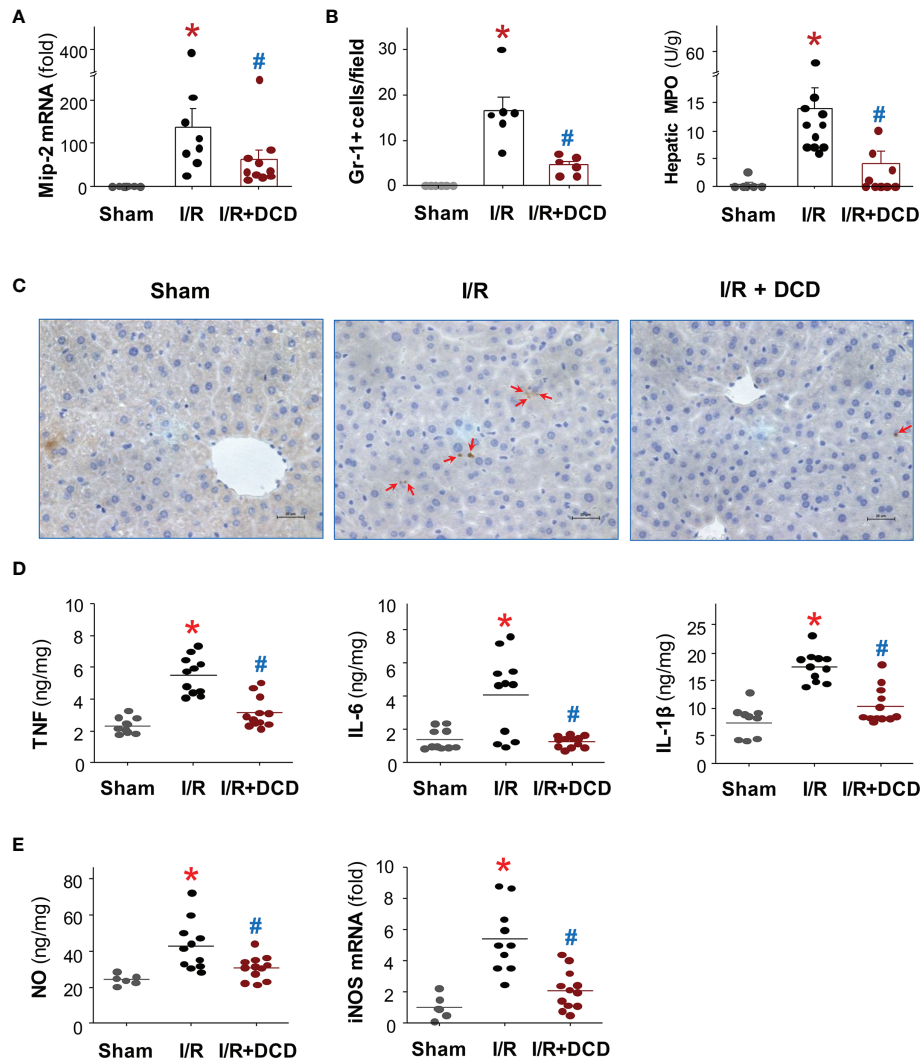


FIGURE 3 | Recombinant DCD attenuated hepatic I/R-induced local inflammation. Male C57BL/6 mice were subjected to hepatic ischemia for 60 min, and treated with control vehicle or DCD solution (0.5 mg/kg) at the beginning of the reperfusion. At 24 h post the onset of reperfusion, the liver tissue was subjected to assays of Mip-2 mRNA expression (**A**), neutrophil infiltration (**B, C**), as well as production of proinflammatory cytokines (**D**) and nitric oxide (NO, **E**), as well as expression of inducible nitric oxide synthase (iNOS, **E**). Data were compared by parametric one-way ANOVA followed by the Fisher Least Significant Difference (LSD) *post hoc* test. * $P < 0.05$ versus "Sham"; # $P < 0.05$ versus "I/R" group.

associated with a significant increase in histological lung injury scores (**Figure 4B**), as well as a parallel increase in lung neutrophil infiltration (**Figures 4C, D**). However, the hepatic I/R-elicited lung neutrophil infiltration and inflammatory injury was similarly and significantly inhibited by DCD administration (**Figures 4A–D**), suggesting that DCD conferred significant protection against lethal hepatic I/R by attenuating both local and remote inflammatory injuries.

DCD Interacted With EGFR and Suppressed the Hepatic I/R-Induced EGFR Phosphorylation

The epidermal growth factor receptor (EGFR) signaling has been suggested as a key regulator of the liver response to injury-

elicited inflammation, as well as subsequent hepatocellular proliferation and neoplastic transformation (41). In an animal model of myocardial ischemia, the expression of EGFR in alveolar macrophages was up-regulated (42), and contributed to the expression of proinflammatory cytokines (such as TNF, IL-6, IL-1 β), chemokines (such as CXCL2/MIP-2, MCP-1, and CCL3) and iNOS (42). To gain further insight into the mechanisms by which DCD attenuated hepatic I/R-induced inflammation, we first tested the possibility that DCD interacted with the extracellular domain of EGFR using two Surface Plasmon Resonance (SPR) techniques. By using the Nicoya gold nanoparticle-based OpenSPR, we found that recombinant DCD exhibited a dose-dependent interaction with the extracellular domain of human EGFR (**Figure 5A**) with an

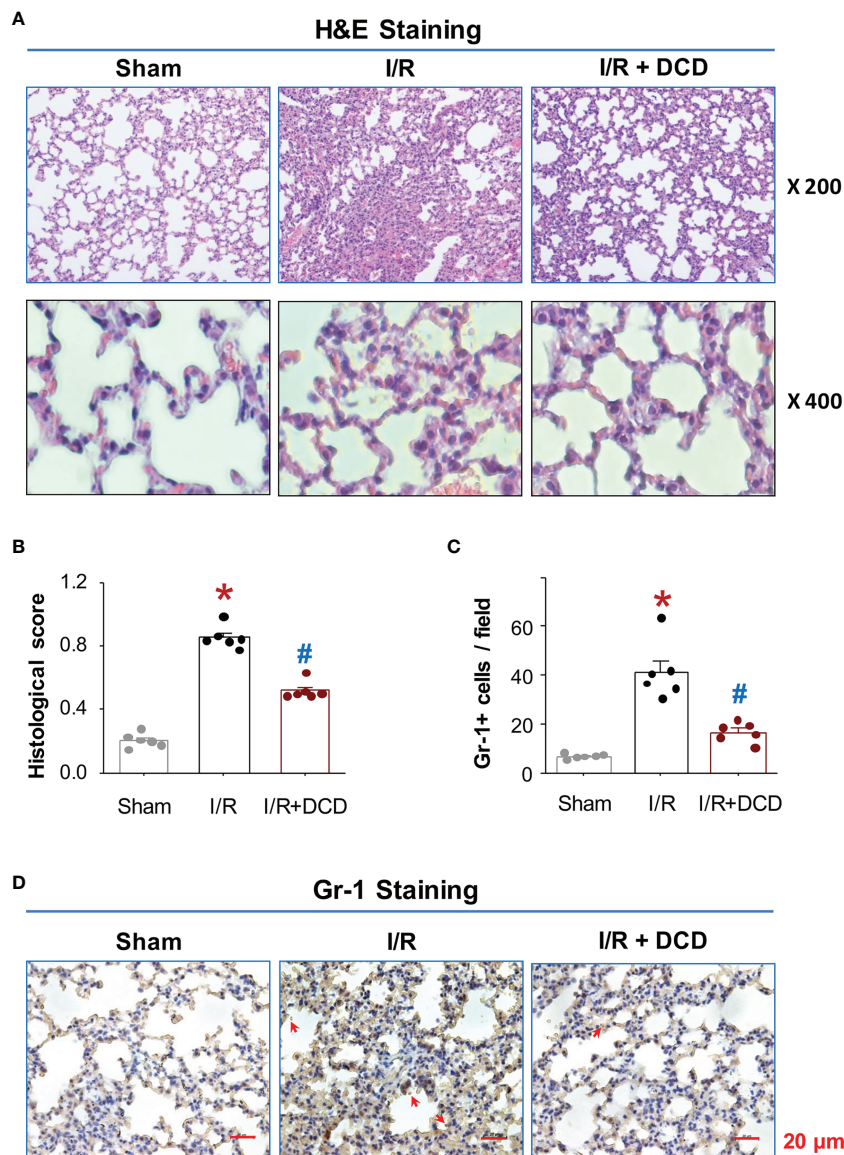


FIGURE 4 | DCD protected mice against hepatic I/R-induced lung injury. **(A)** Histopathological characteristics of lung injury after hepatic I/R. Representative H&E histological images of lung sections at 24 h post the onset of reperfusion. Note a normal lung architecture in the “Sham” control, and extensive lung injury and neutrophil infiltration in the “I/R” group. DCD treatment group (“I/R + DCD”) exhibited a well-preserved tissue structure. **(B)** Histological Scores. Lung injury was assessed histologically using American Thoracic Society Documents’ lung injury scores (with skewed distribution), expressed as means \pm SEM of 6 animals per group, and compared by non-parametric Kruskal-Wallis ANOVA test followed by the Dunn’s *post hoc* test. * $P < 0.05$ vs. “Sham”; # $P < 0.05$ vs. “I/R” group. **(C, D)** Lung neutrophil accumulation. Lung tissue sections were stained with Gr-1-specific antibodies, and the number of Gr-1-positive neutrophils (with normal distribution) per field was expressed as means \pm SEM of 6 animals and compared by parametric one-way ANOVA followed by the Fisher Least Significant Difference (LSD) *post hoc* test **(C)**. * $P < 0.05$ vs. sham; # $P < 0.05$ vs. “I/R” group. Shown in Panel D were representative immunohistological staining of Gr-1-positive neutrophils (pointed by arrows) in lung sections.

equilibrium dissociation constant K_D of 58.1 ± 29.6 nM, as averaged from three independent experiments. In agreement with the minor difference between the side chains of residue 34 of DCD and DCD-C34S (i.e., “-SH group” versus “-OH group”, **Figure 1A**), these two proteins displayed almost identical binding affinities to EGFR ($K_D = 58.1$ nM for DCD versus $K_D = 57.9$ nM for DCD-C34S; **Figure 5A**). To further confirm

this interaction, we also used the traditional Biacore SPR technique, and obtained an essentially similar K_D (58.8 nM, **Figure 5B**) for DCD-EGFR interaction, confirming that DCD and DCD-C34S analog interact with EGFR with similar affinities.

We then examined whether DCD administration affected hepatic I/R-induced phosphorylation of EGFR as well as a downstream signaling molecule, AKT, in the liver tissue.

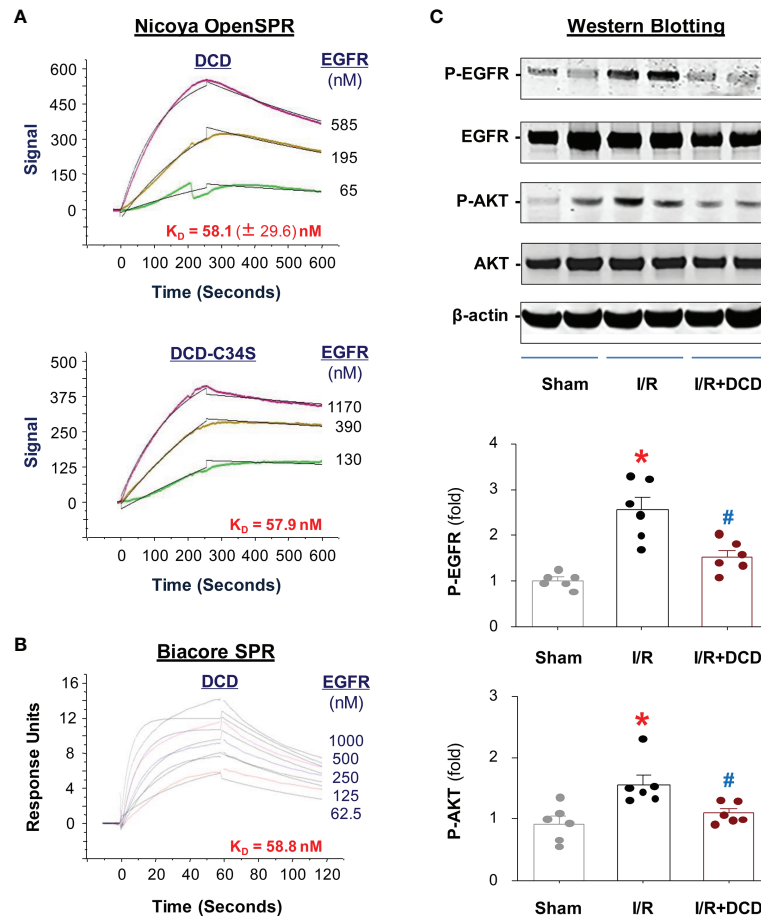


FIGURE 5 | DCD interacted with EGFR and impaired I/R-induced EGFR phosphorylation in the liver. **(A)** Analysis of DCD-EGFR interaction using Nicoya Lifesciences OpenSPR. Highly purified DCD or DCD-C34S was immobilized on a NTA sensor chip, and recombinant protein corresponding to the extracellular domain of human EGFR (residue 25-645) was applied as analyte at various concentrations to estimate the dissociation equilibrium constant (K_D). Shown in the graphs was the K_D (as mean \pm SEM) of 1-3 independent experiments ($n = 3$, Upper Panel; $n = 1$, Lower Panel). **(B)** Analysis of DCD-EGFR interaction using Biacore SPR. Recombinant DCD was immobilized on CM5 chip, and the extracellular domain of human EGFR (residue 25-645) was applied as analyte at 5 different concentrations to estimate the equilibrium dissociation constant K_D . **(C)** DCD administration attenuated hepatic I/R-induced phosphorylation of EGFR and AKT in the liver. Male C57BL/6 mice were subjected to hepatic ischemia and treated with control vehicle or DCD solution (0.5 mg/kg) at the beginning of the reperfusion. At 24 h post the onset of reperfusion, the liver tissue was subjected to Western blotting analysis of total and phosphorylated EGFR ("EGFR" and "P-EGFR") and AKT ("AKT" and "P-AKT"), expressed as % of β -actin (with normal distribution), and compared by parametric one-way ANOVA followed by the Fisher Least Significant Difference (LSD) *post hoc* test. * $P < 0.05$ vs. "Sham"; # $P < 0.05$ vs. "I/R" group.

At 24 h post hepatic I/R, there was a significant increase in the phosphorylation of both EGFR and AKT (**Figure 5C**), although the total levels of EGFR or AKT were not obviously altered at this time point. However, intravenous administration of DCD resulted in a significant inhibition of hepatic I/R-induced phosphorylation of both EGFR and AKT, suggesting a possible role of EGFR signaling in the regulation of DCD-mediated anti-inflammatory actions.

DCD Anti-Inflammatory Activity Required EGFR

To test the role of EGFR in the regulation of DCD-mediated anti-inflammatory actions, we transduced murine macrophage-like

RAW 264.7 cells with lentivirus encoding either vector or Egfr-specific shRNA expression plasmids, and then compared the anti-inflammatory properties of DCD in these divergently transfected cells. In two lines of macrophages (shRNA#21 and shRNA#18) stably transduced by Egfr-specific shRNA plasmid, the constitutive expression level of EGFR was significantly attenuated (**Figure 6A**). Consistent with a previous report (22), recombinant mouse CIRP markedly stimulated macrophages to release nitric oxide (NO, **Figure 6B**), which was dose-dependently inhibited by the co-addition of DCD (**Figure 6B**). However, DCD failed to inhibit the CIRP-induced NO production in these Egfr-specific shRNA-expressing cells (**Figure 6B**), supporting a possible role of EGFR signaling in the regulation of DCD-mediated anti-inflammatory actions.

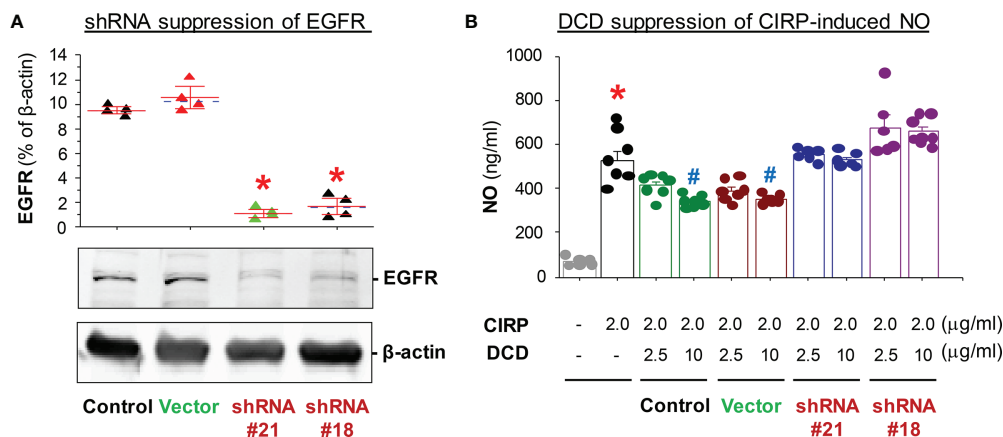


FIGURE 6 | Knock down of EGFR expression impaired DCD-mediated suppression of CIRP-induced NO production in macrophage cultures. **(A)** Expression of EGFR in murine macrophage-like RAW 264.7 cells transfected with vector plasmid ("Vector") or Egfr-specific shRNA-expression plasmid ("shRNA"). Lentivirus carrying vector plasmid ("Vector") or Egfr-specific shRNA expression plasmid ("shRNA") were used to transduce murine macrophage-like RAW 264.7 cells to produce stably transfected cell lines. The relative levels of EGFR in non-transfected controls, or macrophages transfected with vector plasmid ("Vector") or Egfr-specific shRNA-expression plasmid ("shRNA") was determined by Western blotting analysis, expressed as % of β -actin, and compared by parametric one-way ANOVA followed by the Fisher Least Significant Difference (LSD) *post hoc* test. * $P < 0.05$ vs. "Control". **(B)** Effect of DCD on CIRP-induced NO production by macrophages transfected with different plasmids. Non-transfected RAW 264.7 cells ("Control") or cells transfected with vector plasmid ("Vector") or Egfr-specific shRNA ("shRNA #21" or "shRNA #18") were stimulated with recombinant CIRP in the absence or presence of DCD at indicated concentration for 16 h, the level of NO in the culture medium was determined, and compared by parametric one-way ANOVA followed by the Fisher Least Significant Difference (LSD) *post hoc* test. * $P < 0.05$ vs. negative control ("-CIRP-DCD"); # $P < 0.05$ vs. positive control ("+CIRP" alone).

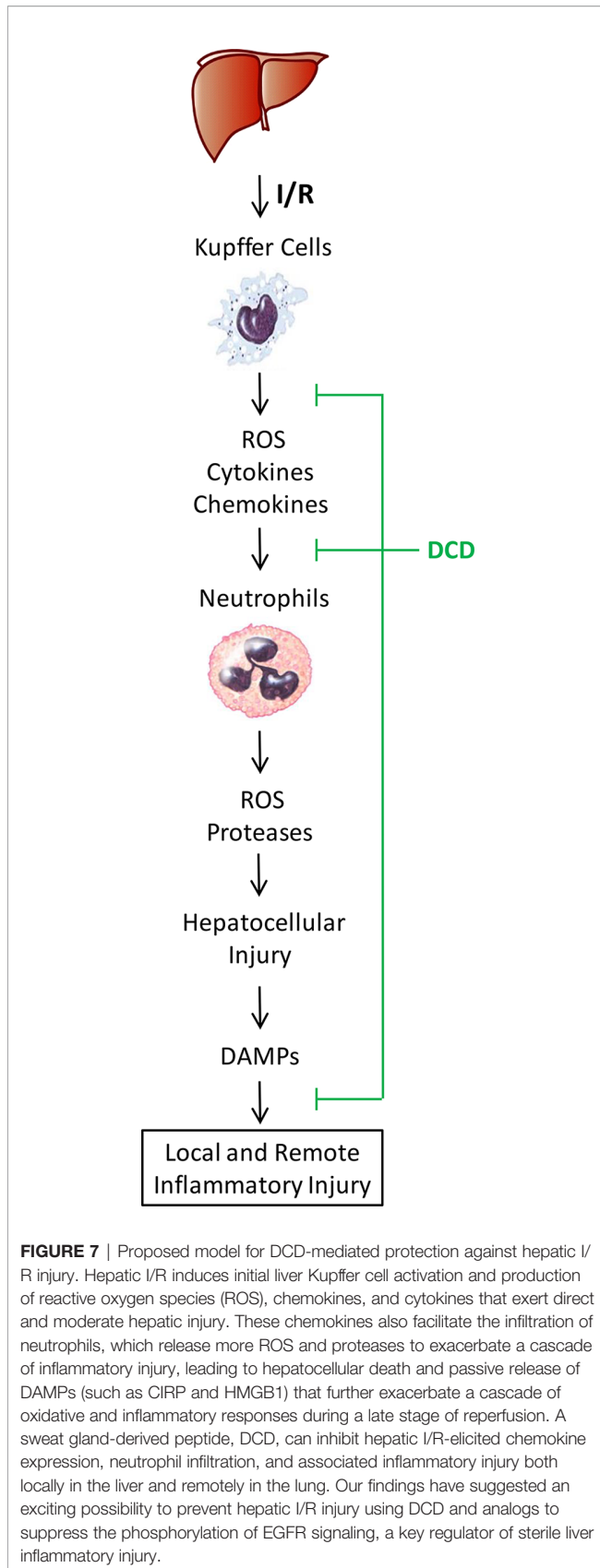
DISCUSSION

Hepatic I/R injury is an unavoidable consequence of major liver surgery and transplantation, and is mediated by sterile inflammatory responses jeopardizing the viability and function of multiple organs. It begins with initial hypoxic insult to ischemic tissues to cause moderate cellular damage (2–4), and continues with subsequent oxidative and inflammatory injury exacerbated by DAMPs such as CIRP (5) and HMGB1 (6, 7) during a late stage of reperfusion (1). Currently, there are no effective therapies to prevent hepatic I/R injury other than ischemic preconditioning and other preventive strategies (43). Thus, the primary objective of the current study was to explore the therapeutic efficacy and protective mechanisms of human DCD using a murine model of hepatic I/R injury. We demonstrated that treatment with recombinant DCD or a DCD-C34S analog conferred similar protection against lethal hepatic I/R, and concurrently attenuated hepatic I/R-elicited inflammatory injury both locally in the liver and remotely in the lung (Figure 7). This DCD-mediated protection was partly attributable to the attenuation of I/R-elicited neutrophil infiltration and inflammatory responses possibly through inhibiting I/R-induced EGFR signaling.

In response to hepatic I/R, liver resident Kupffer cells and infiltrated neutrophils orchestrate rigorous inflammatory responses manifested by the production of ROS, RNS, chemokines, and cytokines that collectively contribute to hepatic injury (1–3). Consequently, hepatocellular injury caused the passive release of DAMPs such as CIRP (5) and HMGB1 (6, 7), which further stimulate a feed-forward cycle of inflammatory injuries

(8, 9) (Figure 7). In response to injury, a neutrophilic CXC chemokine, MIP-2, can be produced by macrophages and hepatocytes, and facilitate neutrophil recruitment and activation (44). Consistent with the role of CXC chemokines in mediating hepatic I/R-elicited deleterious inflammatory responses (45), we found a marked upregulation of Mip-2 expression in ischemic liver tissues. However, at the dose that conferred significant protection against lethal hepatic I/R, DCD also significantly attenuated hepatic I/R-elicited Mip-2 upregulation, and consequently reduced the infiltration of Gr-1-positive neutrophils into ischemic liver tissues. Collectively, these findings have suggested that DCD confers protection against hepatic I/R partly by attenuating neutrophil infiltration through inhibiting the expression of a key neutrophilic chemokine, MIP-2.

In agreement with the important contribution of neutrophil infiltration to I/R-elicited inflammatory IR injury (46), we observed a marked elevation of various proinflammatory cytokines (such as TNF, IL-1 β , and IL-6) and reactive nitrogen species (NO) in the ischemic liver tissues. It has been shown that the inducible nitric oxide synthase (iNOS) responsible for the production of reactive nitrogen species (NO) is synergistically upregulated by various proinflammatory cytokines such as TNF and IL-1 β in the liver (47). Consistently, we found that DCD administration led to a parallel reduction of TNF, IL-1 β , and NO, which was associated with a concurrent reduction of hepatic I/R-elicited iNOS upregulation. Our findings fully support the notion that excessive production of cytotoxic cytokines and NO may escalate severe liver injury (48), and suggest that the sweat gland-derived peptide DCD and its analogs could be developed to pharmacologically modulate injurious inflammatory responses.



It is known that hepatic I/R injury often causes remote tissue inflammatory injury as characterized by the induction of a cascade of proinflammatory mediators that culminates in the recruitment of leukocytes to remote tissues (38). Furthermore, the hepatic I/R-elicited remote tissue inflammatory injury and organ dysfunctions may similarly contribute to the lethal sequelae (38–40). Consistently, we found that hepatic I/R induced a marked lung inflammatory injury, as judged by the elevated neutrophil infiltration and pathological alterations of lung histology such as alveolar septal wall thickening, leukocyte infiltration, and alveolar congestion. However, the administration of DCD at the beginning of reperfusion resulted in a significant attenuation of the hepatic I/R-elicited lung inflammatory injury. Our findings that intravenous administration of DCD concurrently reduced liver and lung damage in both organs fully support the therapeutic potential of various anti-inflammatory agents in attenuating hepatic I/R-elicited multiple organ dysfunctions (43, 49, 50).

In addition, our current observations that DCD significantly attenuated hepatic I/R-elicited inflammatory response *in vivo* fully support our previous report that DCD differentially modulates the production of various cytokines/chemokines *in vitro* (22). Our present study also supports the notion that excessive release of DAMPs and excessive inflammation may further exacerbate the severity of hepatic I/R injury (51), although appropriate inflammatory responses might still be needed to facilitate tissue repair and promotes the re-establishment of homeostasis. The mechanism by which DCD suppresses inflammatory responses remains an exciting subject of future investigation. However, it is partly attributable to its possible inhibition of EGFR signaling, a key pathway implicated in the regulation of injury-elicited inflammatory responses in the liver (41, 42). First, Surface Plasmon Resonance analyses revealed that DCD could bind to the extracellular domain of EGFR with high affinities. Second, intravenous administration of DCD resulted in a significant suppression of hepatic I/R-elicited phosphorylation of EGFR, as well as a downstream kinase, AKT (35). Finally, the possible role of EGFR in the regulation of DCD-mediated anti-inflammatory activities was confirmed by knocking down the expression of EGFR by transfection with plasmids encoding for specific shRNA, which not only reduced Egr expression, but also abrogated the DCD-mediated inhibition of NO production induced by a DAMP, CIRP. Collectively, these findings have suggested that DCD confers protection against lethal hepatic I/R partly through inhibiting EGFR signaling.

Our current study also has several obvious limitations. 1) We have not yet tried other routes of administration, and thus do not know whether DCD confers a similar protection if given *via* other routes of administration. 2) It is not yet known whether DCD administration affects hepatic I/R-induced expression of anti-inflammatory cytokines (e.g., IL-37 and IL-1Ra) in pre-clinical and clinical settings. 3) The intricate molecular mechanisms by which DCD divergently modulates the I/R-induced production of different cytokines and chemokines were not investigated in the present study. 4) It is presently not yet known whether genetically

silencing EGFR would abrogate the activation and phosphorylation of various downstream signaling kinases (e.g., AKT and ERK) in murine macrophage cultures. In conclusion, our present study suggests that treatment with human DCD or DCD-C34S analog can potentially be developed as novel therapeutic strategies for hepatic I/R injury. The DCD-mediated protection was associated with a significant reduction in inflammatory injury both locally in the liver and remotely in the lung tissue, as manifested by the attenuation of neutrophil infiltration and production of proinflammatory cytokines. The anti-inflammatory action of DCD was partly dependent on its inhibition of EGFR signaling. Collectively, the present study suggests that the sweat gland-derived peptide DCD or its analogs might be developed as potential therapeutic agents to attenuate hepatic I/R-induced inflammation and tissue injury potentially by impairing EGFR signaling. Although it is not yet known whether our rodent model of acute hepatic I/R truly mimics human liver transplantation-associated I/R, we predict that DCD and DCD-C34S are likely protective against liver transplantation-associated I/R and inflammation in clinical settings.

DATA AVAILABILITY STATEMENT

The raw data supporting the conclusions of this article will be made available by the authors, without undue reservation.

ETHICS STATEMENT

The animal study was reviewed and approved by the IACUC of the Feinstein Institutes for Medical Research.

REFERENCES

- van Golen RF, Reiniers MJ, Olthoff PB, van Gulik TM, Heger M. Sterile Inflammation in Hepatic Ischemia/Reperfusion Injury: Present Concepts and Potential Therapeutics. *J Gastroenterol Hepatol* (2013) 28:394–400. doi: 10.1111/jgh.12072
- Okaya T, Lentsch AB. Cytokine Cascades and the Hepatic Inflammatory Response to Ischemia and Reperfusion. *J Invest Surg* (2003) 16:141–7. doi: 10.1080/08941930390205782
- Ahmed O, Robinson MW, O'Farrelly C. Inflammatory Processes in the Liver: Divergent Roles in Homeostasis and Pathology. *Cell Mol Immunol* (2021) 18:1375–86. doi: 10.1038/s41423-021-00639-2
- Abu-Amara M, Yang SY, Tapuria N, Fuller B, Davidson B, Seifalian A. Liver Ischemia/Reperfusion Injury: Processes in Inflammatory Networks—A Review. *Liver Transpl* (2010) 16:1016–32. doi: 10.1002/lt.22117
- Qiang X, Yang WL, Wu R, Zhou M, Jacob A, Dong W, et al. Cold-Inducible RNA-Binding Protein (CIRP) Triggers Inflammatory Responses in Hemorrhagic Shock and Sepsis. *Nat Med* (2013) 19:1489–95. doi: 10.1038/nm.3368
- Wang H, Bloom O, Zhang M, Vishnubhakat JM, Ombrellino M, Che J, et al. HMGB-1 As a Late Mediator of Endotoxin Lethality in Mice. *Science* (1999) 285:248–51. doi: 10.1126/science.285.5425.248
- Zhu CS, Wang W, Qiang X, Chen W, Lan X, Li J, et al. Endogenous Regulation and Pharmacological Modulation of Sepsis-Induced HMGB1 Release and Action: An Updated Review. *Cells* (2021) 10:2220. doi: 10.3390/cells10092220

AUTHOR CONTRIBUTIONS

XQ performed all animal experiments, and generated a rough draft of the manuscript. JL and KT generated recombinant DCD and DCD-C34S analog for the present study. MH and YA-A performed Biacore SPR analysis of DCD-EGFR interaction. SZ performed Open SPR analysis of DCD-EGFR interaction. WC was involved in some cellular experiments. PW supervised the animal study, interpreted some results, and together with MB, edited the manuscript. HW supervised the cellular and biochemical studies, interpreted most of the results, generated the final figures, significantly revised and finalized the manuscript. All authors read and approved the submitted version.

FUNDING

This work was supported in part by the National Institutes of Health (NIH) grants R01GM063075 (to HW), R01AT005076 (to HW), R35GM118337 (to PW), and R01HL076179 (to PW). The Biacore T200 instrument was purchased with a NIH capital equipment grant (1S10RR033072 to YA-A).

ACKNOWLEDGMENTS

We would like to thank Dr. Yongjun Wang, a former member of HW's lab, for his technical assistance in establishing stable macrophage cell lines that express control vector or EGFR-specific shRNA expression plasmids. We would also like to thank Dr. Mahendar Ochani, a former member of PW's lab, for his technical assistance in establishing the murine model of hepatic ischemia-reperfusion injury for the present study.

- Tsung A, Sahai R, Tanaka H, Nakao A, Fink MP, Lotze MT, et al. The Nuclear Factor HMGB1 Mediates Hepatic Injury After Murine Liver Ischemia-Reperfusion. *J Exp Med* (2005) 201:1135–43. doi: 10.1084/jem.20042614
- Godwin A, Yang WL, Sharma A, Khader A, Wang Z, Zhang F, et al. Blocking Cold-Inducible RNA-Binding Protein Protects Liver From Ischemia-Reperfusion Injury. *Shock* (2015) 43:24–30. doi: 10.1097/SHK.0000000000000251
- Lu L, Zhou H, Ni M, Wang X, Busuttill R, Kupiec-Weglinski J, et al. Innate Immune Regulations and Liver Ischemia-Reperfusion Injury. *Transplantation* (2016) 100:2601–10. doi: 10.1097/TP.0000000000001411
- Zhai Y, Petrowsky H, Hong JC, Busuttill RW, Kupiec-Weglinski JW. Ischaemia-Reperfusion Injury in Liver Transplantation—From Bench to Bedside. *Nat Rev Gastroenterol Hepatol* (2013) 10:79–89. doi: 10.1038/nrgastro.2012.225
- Schitteck B, Hipfel R, Sauer B, Bauer J, Kalbacher H, Stevanovic S, et al. Dermcidin: A Novel Human Antibiotic Peptide Secreted by Sweat Glands. *Nat Immunol* (2001) 2:1133–7. doi: 10.1038/ni732
- Rieg S, Seeber S, Steffen H, Humeny A, Kalbacher H, Stevanovic S, et al. Generation of Multiple Stable Dermcidin-Derived Antimicrobial Peptides in Sweat of Different Body Sites. *J Invest Dermatol* (2006) 126:354–65. doi: 10.1038/sj.jid.5700041
- Schitteck B. The Multiple Facets of Dermcidin in Cell Survival and Host Defense. *J Innate Immun* (2012) 4:349–60. doi: 10.1159/000336844
- Li M, Rigby K, Lai Y, Nair V, Peschel A, Schitteck B, et al. Staphylococcus Aureus Mutant Screen Reveals Interaction of the Human Antimicrobial Peptide Dermcidin With Membrane Phospholipids. *Antimicrob Agents Chemother* (2009) 53:4200–10. doi: 10.1128/AAC.00428-09

16. Burian M, Schittek B. The Secrets of Dermcidin Action. *Int J Med Microbiol* (2015) 305:283–6. doi: 10.1016/j.ijmm.2014.12.012
17. Stewart GD, Lowrie AG, Riddick AC, Fearon KC, Habib FK, Ross JA. Dermcidin Expression Confers a Survival Advantage in Prostate Cancer Cells Subjected to Oxidative Stress or Hypoxia. *Prostate* (2007) 67:1308–17. doi: 10.1002/pros.20618
18. Lousada MB, Lachnit T, Edelkamp J, Rouill   T, Ajdic D, Uchida Y, et al. Exploring the Human Hair Follicle Microbiome. *Br J Dermatol* (2021) 184:802–15. doi: 10.1111/bjd.19461
19. Niyonsaba F, Kiatsurayanon C, Chieosilapatham P, Ogawa H. Friends or Foes? Host Defense (Antimicrobial) Peptides and Proteins in Human Skin Diseases. *Exp Dermatol* (2017) 26:989–98. doi: 10.1111/exd.13314
20. Rieg S, Steffen H, Seeber S, Humeny A, Kalbacher H, Dietz K, et al. Deficiency of Dermcidin-Derived Antimicrobial Peptides in Sweat of Patients With Atopic Dermatitis Correlates With an Impaired Innate Defense of Human Skin in Vivo. *J Immunol* (2005) 174:8003–10. doi: 10.4049/jimmunol.174.12.8003
21. Pathak S, De Souza GA, Salte T, Wiker HG, Asjo B. HIV Induces Both a Down-Regulation of IRAK-4 That Impairs TLR Signalling and an Up-Regulation of the Antibiotic Peptide Dermcidin in Monocytic Cells. *Scand J Immunol* (2009) 70:264–76. doi: 10.1111/j.1365-3083.2009.02299.x
22. Wang E, Qiang X, Li J, Zhu S, Wang P. The in Vitro Immune-Modulating Properties of a Sweat Gland-Derived Antimicrobial Peptide Dermcidin. *Shock* (2016) 45:28–32. doi: 10.1097/SHK.0000000000000488
23. Khader A, Yang WL, Godwin A, Prince JM, Nicastro JM, Coppa GF, et al. Sirtuin 1 Stimulation Attenuates Ischemic Liver Injury and Enhances Mitochondrial Recovery and Autophagy. *Crit Care Med* (2016) 44:e651–63. doi: 10.1097/CCM.0000000000001637
24. Wang Y, Wong GT, Man K, Irwin MG. Pretreatment With Intrathecal or Intravenous Morphine Attenuates Hepatic Ischaemia-Reperfusion Injury in Normal and Cirrhotic Rat Liver. *Br J Anaesth* (2012) 109:529–39. doi: 10.1093/bja/aes209
25. Liu X, Yang H, Liu Y, Jiao Y, Yang L, Wang X, et al. Remifentanyl Upregulates Hepatic IL-18 Binding Protein (IL-18bp) Expression Through Transcriptional Control. *Lab Invest* (2018) 98:1588–99. doi: 10.1038/s41374-018-0111-y
26. Yang LQ, Tao KM, Liu YT, Cheung CW, Irwin MG, Wong GT, et al. Remifentanyl Preconditioning Reduces Hepatic Ischemia-Reperfusion Injury in Rats Via Inducible Nitric Oxide Synthase Expression. *Anesthesiology* (2011) 114:1036–47. doi: 10.1097/ALN.0b013e3182104956
27. Letson HL, Dobson GP. Buprenorphine Analgesia Reduces Survival With ALM Resuscitation in a Rat Model of Uncontrolled Hemorrhage: Concerns for Trauma-Related Research. *Shock* (2021) 55:379–87. doi: 10.1097/SHK.0000000000001630
28. Chen W, Brenner M, Aziz M, Chavan SS, Deutschman CS, Diamond B, et al. Buprenorphine Markedly Elevates a Panel of Surrogate Markers in a Murine Model of Sepsis. *Shock* (2019) 52:550–3. doi: 10.1097/SHK.0000000000001361
29. Li W, Ashok M, Li J, Yang H, Sama AE, Wang H. A Major Ingredient of Green Tea Rescues Mice From Lethal Sepsis Partly by Inhibiting Hmgb1. *PLoS One* (2007) 2:e1153. doi: 10.1371/journal.pone.0001153
30. Li W, Li J, Ashok M, Wu R, Chen D, Yang L, et al. A Cardiovascular Drug Rescues Mice From Lethal Sepsis by Selectively Attenuating a Late-Acting Proinflammatory Mediator, High Mobility Group Box 1. *J Immunol* (2007) 178:3856–64. doi: 10.4049/jimmunol.178.6.3856
31. Matute-Bello G, Downey G, Moore BB, Groshong SD, Matthay MA, Slutsky AS, et al. An Official American Thoracic Society Workshop Report: Features and Measurements of Experimental Acute Lung Injury in Animals. *Am J Respir Cell Mol Biol* (2011) 44:725–38. doi: 10.1165/rcmb.2009-0210ST
32. Chen W, Qiang X, Wang Y, Zhu S, Li J, Babaev A, et al. Identification of Tetranection-Targeting Monoclonal Antibodies to Treat Potentially Lethal Sepsis. *Sci Transl Med* (2020) 12:12–539. doi: 10.1126/scitranslmed.aaz3833
33. Qiang X, Zhu S, Li J, Chen W, Yang H, Wang P, et al. Monoclonal Antibodies Capable of Binding SARS-CoV-2 Spike Protein Receptor-Binding Motif Specifically Prevent GM-CSF Induction. *J Leukoc Biol* (2022) 111:261–7. doi: 10.1002/JLB.3COVCRA0920-628RR
34. Yang H, Wang H, Wang Y, Addorisio M, Li J, Postiglione MJ, et al. The Haptoglobin Beta Subunit Sequesters HMGB1 Toxicity in Sterile and Infectious Inflammation. *J Intern Med* (2017) 282:76–93. doi: 10.1111/joim.12619
35. Li W, Li J, Sama AE, Wang H. Carbenoxolone Blocks Endotoxin-Induced Protein Kinase R (PKR) Activation and High Mobility Group Box 1 (HMGB1) Release. *Mol Med* (2013) 19:203–11. doi: 10.2119/molmed.2013.00064
36. Zhu S, Ashok M, Li J, Li W, Yang H, Wang P, et al. Spermine Protects Mice Against Lethal Sepsis Partly by Attenuating Surrogate Inflammatory Markers. *Mol Med* (2009) 15:275–82. doi: 10.2119/molmed.2009.00062
37. Nakano T, Yoshino T, Fujimura T, Arai S, Mukuno A, Sato N, et al. Reduced Expression of Dermcidin, a Peptide Active Against Propionibacterium Acnes, in Sweat of Patients With Acne Vulgaris. *Acta Derm Venereol* (2015) 95:783–6. doi: 10.2340/00015555-2068
38. Husted TL, Lentsch AB. The Role of Cytokines in Pharmacological Modulation of Hepatic Ischemia/Reperfusion Injury. *Curr Pharm Des* (2006) 12:2867–73. doi: 10.2174/13816120677947597
39. Zhang H, Goswami J, Varley P, van der Windt DJ, Ren J, Loughran P, et al. Hepatic Surgical Stress Promotes Systemic Immunothrombosis That Results in Distant Organ Injury. *Front Immunol* (2020) 11:987. doi: 10.3389/fimmu.2020.00987
40. Cannistr   M, Ruggiero M, Zullo A, Gallelli G, Serafini S, Maria M, et al. Hepatic Ischemia Reperfusion Injury: A Systematic Review of Literature and the Role of Current Drugs and Biomarkers. *Int J Surg* (2016) 33 Suppl 1:S57–70. doi: 10.1016/j.ijssu.2016.05.050
41. Berasain C, Avila MA. The EGFR Signalling System in the Liver: From Hepatoprotection to Hepatocarcinogenesis. *J Gastroenterol* (2014) 49:9–23. doi: 10.1007/s00535-013-0907-x
42. Hoyer FF, Naxerova K, Schloss MJ, Hulsmans M, Nair AV, Dutta P, et al. Tissue-Specific Macrophage Responses to Remote Injury Impact the Outcome of Subsequent Local Immune Challenge. *Immunity* (2019) 51:899–914. doi: 10.1016/j.immuni.2019.10.010
43. Selzner N, Rudiger H, Graf R, Clavien PA. Protective Strategies Against Ischemic Injury of the Liver. *Gastroenterology* (2003) 125:917–36. doi: 10.1016/S0016-5085(03)01048-5
44. Qin CC, Liu YN, Hu Y, Yang Y, Chen Z. Macrophage Inflammatory Protein-2 As Mediator of Inflammation in Acute Liver Injury. *World J Gastroenterol* (2017) 23:3043–52. doi: 10.3748/wjg.v23.i17.3043
45. Clarke CN, Kuboki S, Tevar A, Lentsch AB, Edwards M. CXC Chemokines Play a Critical Role in Liver Injury, Recovery, and Regeneration. *Am J Surg* (2009) 198:415–9. doi: 10.1016/j.amjsurg.2009.01.025
46. Oliveira THC, Marques PE, Proost P, Teixeira MMM. Neutrophils: A Cornerstone of Liver Ischemia and Reperfusion Injury. *Lab Invest* (2018) 98:51–62. doi: 10.1038/labinvest.2017.90
47. Taylor BS, Alarcon LH, Billiar TR. Inducible Nitric Oxide Synthase in the Liver: Regulation and Function. *Biochem (Mosc)* (1998) 63:766–81.
48. Hon WM, Lee KH, Khoo HE. Nitric Oxide in Liver Diseases: Friend, Foe, or Just Passerby? *Ann NY Acad Sci* (2002) 962:275–95. doi: 10.1111/j.1749-6632.2002.tb04074.x.275-295
49. Hato S, Urakami A, Yamano T, Uemura T, Ota T, Hirai R, et al. Attenuation of Liver and Lung Injury After Hepatic Ischemia and Reperfusion by a Cytokine-Suppressive Agent, Fr167653. *Eur Surg Res* (2001) 33:202–9. doi: 10.1159/000049707
50. Lentsch AB, Yoshidome H, Warner RL, Ward PA, Edwards MJ. Secretory Leukocyte Protease Inhibitor in Mice Regulates Local and Remote Organ Inflammatory Injury Induced by Hepatic Ischemia/Reperfusion. *Gastroenterology* (1999) 117:953–61. doi: 10.1016/S0016-5085(99)70355-0
51. Brenner C, Galluzzi L, Kepp O, Kroemer G. Decoding Cell Death Signals in Liver Inflammation. *J Hepatol* (2013) 59:583–94. doi: 10.1016/j.jhep.2013.03.033

Conflict of Interest: PW and HW are co-inventors of a patent entitled “Use of dermcidin in sterile anti-inflammatory conditions” (US15/769,800). PW is a co-founder of TheraSource LLC, which has an option to license the relevant technology. MB is a part-time employee of TheraSource LLC.

The remaining authors declare that the research was conducted in the absence of any commercial or financial relationships that could be construed as a potential conflict of interest.

Publisher’s Note: All claims expressed in this article are solely those of the authors and do not necessarily represent those of their affiliated organizations, or those of the publisher, the editors and the reviewers. Any product that may be evaluated in

this article, or claim that may be made by its manufacturer, is not guaranteed or endorsed by the publisher.

Copyright © 2022 Qiang, Li, Zhu, He, Chen, Al-Abed, Brenner, Tracey, Wang and Wang. This is an open-access article distributed under the terms of the Creative

Commons Attribution License (CC BY). The use, distribution or reproduction in other forums is permitted, provided the original author(s) and the copyright owner(s) are credited and that the original publication in this journal is cited, in accordance with accepted academic practice. No use, distribution or reproduction is permitted which does not comply with these terms.